

RESEARCH

Open Access



# ATF3 mediates PM2.5-induced apoptosis and inflammation in ovarian granulosa cells

Xiandan Zhang<sup>1†</sup>, Xuan Wang<sup>2†</sup>, Hao Li<sup>3†</sup>, Haihong Wang<sup>4</sup>, Dewei Du<sup>1</sup> and Huijuan Huang<sup>4\*</sup>

## Abstract

Particulate matter 2.5 (PM2.5) pollution has emerged as a major global public health concern because of its adverse effects on human health. Our group has previously demonstrated that PM2.5 exposure can seriously impair ovarian function. However, the underlying mechanisms remain a mystery. This study verifies ovarian damage in mice, evidenced by inflammatory cell infiltration and follicular atresia, following 5 months of PM2.5 exposure via tracheal drip (35  $\mu\text{g}/\text{m}^3$  for low dose and 150  $\mu\text{g}/\text{m}^3$  for high dose). In addition, PM2.5 exposure inhibited the cell viability of human granulosa cells (KGN) and induced apoptosis at the concentrations of 50, 100, and 150  $\mu\text{g}/\text{mL}$  for 24 h. The apoptosis of KGN cells induced by inflammation contributes to follicular atresia. Furthermore, we conducted RNA-sequencing analysis to identify the genes and pathways triggered by PM2.5 (100  $\mu\text{g}/\text{mL}$ ) exposure, which decreases the KGN cell viability. We found a significant increase in Activating Transcription Factor 3 (ATF3). Further mechanistic studies reveal a strong association between PM2.5-induced apoptosis, inflammation, and ATF3 with its downstream oxidative stress signals. In summary, the ATF3 pathway serves a vital role in the ovarian injury caused by PM2.5 exposures.

**Keywords** PM2.5, Apoptosis, Inflammation, ATF3, Ovarian function

## Introduction

Recently, air pollution has become the fifth leading risk factor for non-contagious disease deaths, contributing to 5.6 million deaths in the world. Among pollutants, ambient fine particulate matter (PM2.5, with a diameter  $\leq 2.5 \mu\text{m}$ ) poses the greatest concern [1]. The primary

sources of PM2.5 are vehicle emissions and industrial fuel combustion, which release organic matter, nitrate, ammonium, and sulfate [2, 3]. PM2.5 poses a significant threat to human health due to its ability to be deposited in the alveoli via the nasal cavity and trachea, and to enter the bloodstream through the pulmonary and vascular barriers [4, 5]. Previous studies have established a clear link between PM2.5 exposure and rising incidence of various diseases. Epidemiological investigations indicate that for every 10  $\mu\text{g}/\text{m}^3$  increase in the average daily concentration of PM2.5 in China, the total daily non-accidental death rate rises by 17%<sup>2</sup>. Worse than death, women exposed to PM2.5 face increased risks of endocrine dysfunction, prolonged menstrual cycles, decreased ovarian function, and reduced pregnancy rates [6–9]. Asa Naav showed that PM2.5 exposure decreases levels of Human Chorionic Gonadotropin (hCG) [10], ultimately affecting placental function, and increasing the

<sup>†</sup>Xiandan Zhang, Xuan Wang and Hao Li contributed equally to this work.

\*Correspondence:

Huijuan Huang  
hhj352@163.com

<sup>1</sup>Department of Gynecology and Obstetrics, The University of Hong Kong-Shenzhen Hospital, Shenzhen, China

<sup>2</sup>Department of Dermatology, Lianyungang Municipal Oriental Hospital, Lianyungang, China

<sup>3</sup>College of Life and Science, Xiamen University, Xiamen, China

<sup>4</sup>Department of Gynecology and Obstetrics, The 900 Hospital of the Joint Service Support Force of the People's Liberation Army of China, Fuzhou, China



risk of preterm birth [11]. Research has previously shown that PM2.5 exposure leads to decreased levels of Estradiol (E2), Progesterone (P), and Anti-Müllerian Hormone (AMH), and increased levels of Follicle Stimulating Hormone (FSH). It also significantly increases atretic follicles, altering the ultrastructure of ovarian germ cells and damaging ovarian function in various ways. However, the specific mechanism by which PM2.5 affects the female reproductive system remains unclear.

Previous studies showed that there is a strong relationship between PM2.5 and occurrence of apoptosis and inflammation. Yin reported that in the cardiovascular system, PM2.5 can activate the Cyclooxygenase-2/Prostaglandin E Synthase/Prostaglandin E2 (COX-2/PGES/PGE2) inflammatory pathway in vascular endothelial cells, leading to increased apoptosis and inflammatory responses [12]. Cao showed that PM2.5 induces apoptosis in mouse cardiomyocytes by activating reactive oxygen species (ROS) through the Mitogen-Activated Protein Kinase (MAPK) pathway [13]. PM2.5 exposure not only enhances inflammatory response and oxidative stress but also increases airway hyperresponsiveness, ultimately leading to apoptosis of human bronchial epithelial cells in the respiratory system [14, 15]. However, the detailed cellular and molecular mechanisms through which chronic PM2.5 exposure causes ovarian damage remain largely unaddressed.

Experimental studies have shown that ATF3 is crucial in causing cell inflammation and apoptosis [16]. Under physiological conditions, the expression of ATF3 is stimulated by various stress signals, including cytokines, hypoxia, adipokines, and chemokines [17–19]. ATF3, a transcription factor encoded by 181 amino acids with a molecular mass of 22 kDa, belongs to the activated protein 1 (AP-1) family and is classified as a basic leucine zipper (bZip) transcription factor [20]. ATF3's physiological role in various cell types is to alleviate cellular stress by repairing DNA damage. Acute hypoxia-induced Tumor necrosis factor alpha (TNF $\alpha$ ) increases the expression of ATF3 in endothelial cells, inhibiting doxorubicin-induced apoptosis in mouse cardiomyocytes by activating the c-Jun N-terminal Kinase (JNK) pathway [21]. PM2.5 exposure can trigger HEB cell apoptosis, ATF3 upregulation, and the secretion of Interleukin-6 (IL-6) [22]. However, it is unclear whether ATF3 is involved in the PM2.5-induced stress response in ovarian after long-term exposure.

## Results

### Ovarian changes induced by the exposure to PM2.5

PM2.5 can cause menstrual cycle changes and ovarian damage, ultimately leading to a decline in ovarian reserve function, as confirmed by epidemiological and experimental studies [6]. We found that PM2.5 exposure causes

ovarian inflammation in mice. Hematoxylin and eosin (H&E) staining revealed that chronic exposure to PM2.5 led to inflammatory cells infiltrating into the ovary (Fig. 1A). Consistent with previous experimental results, higher concentrations of PM2.5 are associated with an increased proportion of atretic follicles in mice [23]. This indicates that PM2.5 can induce ovarian inflammation and follicular atresia. To confirm PM2.5-induced ovarian damage, we selected the ovarian granulosa cell line KGN as a model. Similarly, PM2.5 concentrations were as follows: 0, 50, 100, 150, 200, and 300  $\mu\text{g}/\text{mL}$ . The cells were co-cultured for 36 h, and cell morphology and viability were observed under a microscope. The granulosa cells showed dose-dependent morphological changes, including a shrunken and elongated structure, indicating that PM2.5 significantly affects granulosa cell activity. (Fig. 1B).

### PM2.5 reduces the growth rate of ovarian granulosa cells, and the cell cycle stays in the S phase

We treated KGN cells with different concentrations of PM2.5 to validate its effect on the cell cycle of granulosa cells. PM2.5 concentrations were as follows: 0, 50, 100, 150, 200, and 300  $\mu\text{g}/\text{mL}$ . The cells were co-cultured for 36 h. As shown in diagrams in Fig. 2A, higher PM2.5 concentrations correlate with lower KGN activity, indicating a clear concentration-dependent trend (Fig. 2A). To determine the effects of continuous PM2.5 exposure on cells, we treated KGN cells with 100  $\mu\text{g}/\text{mL}$  PM2.5. We noticed that the cell viability was rapidly decreased over time. After 48 h treatment, KGN cells almost completely lost their inherent growth rate, whereas control cells maintained their original growth rate (Fig. 2B). Further investigation into the influence of PM2.5 on KGN cells activation mechanisms revealed that KGN cells were primarily blocked in the S phase of the cell cycle after 24 h of treatment with various PM2.5 concentrations. This phenomenon became more pronounced with increasing concentrations (Fig. 2C–D). This data indicate that exposure to PM2.5 can lead to the decreased cell viability and cell cycle arrest in the S phase.

### PM2.5 triggers the apoptosis and inflammatory response of KGN cells

The initiation and exacerbation of inflammation, along with the redox response, are recognized as key outcomes in cells significantly influenced by PM2.5. To elucidate the molecular mechanisms underlying these phenomena, we performed RNA sequencing (RNA-seq) to identify genes and pathways activated by PM2.5 (100  $\mu\text{g}/\text{mL}$ ) exposure, which reduced KGN cell viability. Among 343 differentially expressed genes, 181 were upregulated, and 162 were downregulated. A heat map was generated to visualize the changes in these differentially expressed genes

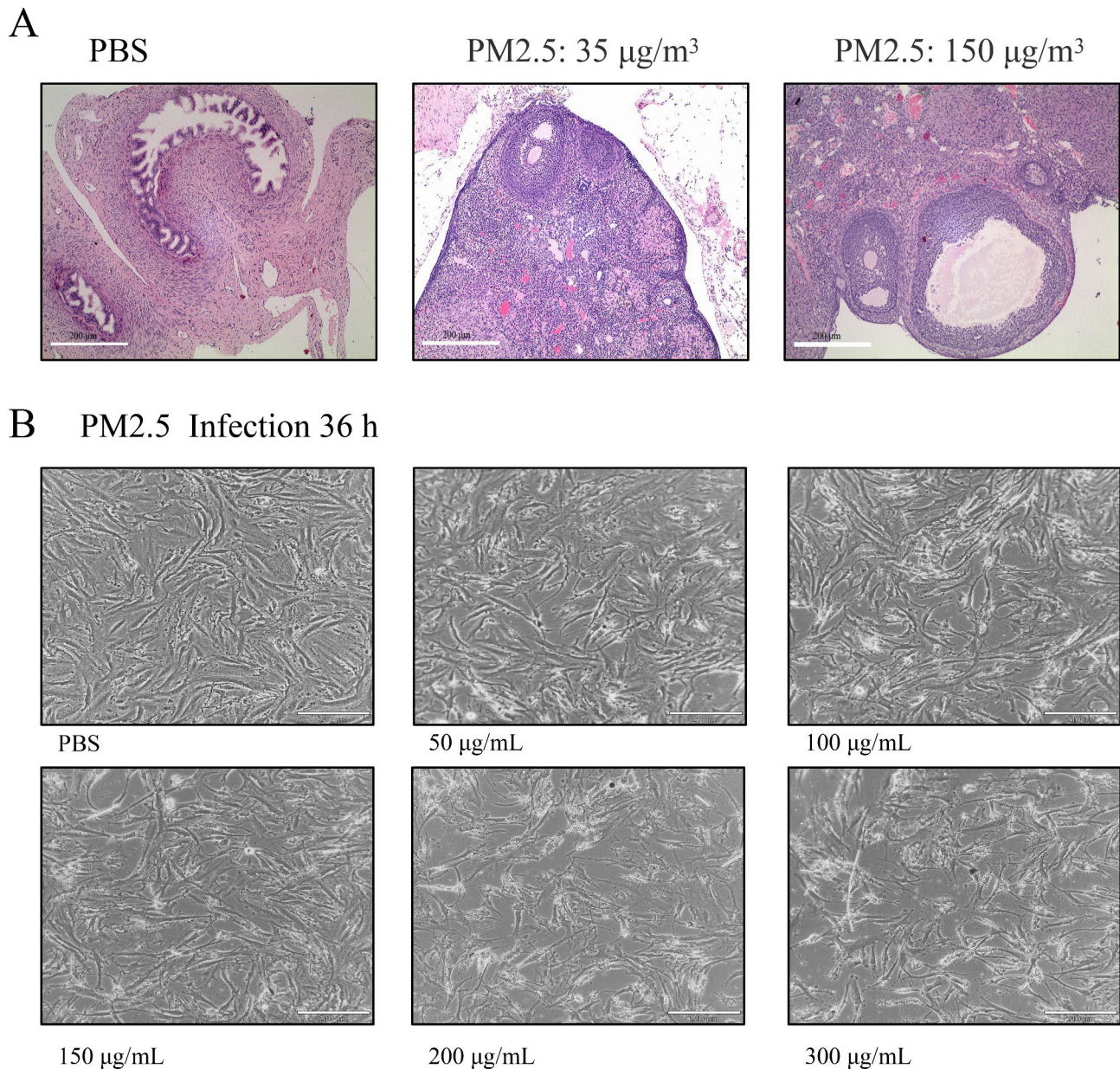


**Fig. 1** PM2.5 exposure aggravated ovarian injury. **(A)** Representative H&E staining images of mouse ovaries following chronic whole-body PM2.5 exposure (200 $\times$ ). **(B)** Different concentrations of PM2.5 exposed KGN cells for 36 h (100 $\times$ )

more clearly (Fig. 3A). To identify the signaling pathways affected by PM2.5 exposure in KGN cells, we further analyzed significantly differentially expressed genes using the Kyoto Encyclopedia of Genes and Genomes (KEGG) and Gene Set Enrichment Analysis (GSEA) (Fig. 3B-D). Comparing with these databases, we discovered that the upregulated genes are primarily involved in pathways causing apoptosis and inflammatory response. As expected, apoptosis was observed in cell samples after 36 h. Furthermore, the rate of apoptosis was concentration-dependent on PM2.5 (Fig. 3E-F). We found that the inflammatory cytokine Interleukin-1 beta (IL-1 $\beta$ ), IL-6

and TNF- $\alpha$  increased 24 h after the PM2.5 treatment (Fig. 3G). To confirm the specific effects of PM2.5 on KGN cells, we used the MitoSOX to detect the ROS in KGN cells. Results demonstrated that 36 h after PM2.5 treatment, ROS levels, indicating oxidative reactions within KGN cells, increased with rising PM2.5 concentration. However, ROS levels did not show a statistically significant increase after 24 h of treatment (Fig. 3H-I). To sum up, PM2.5 aggravates the inflammatory response, induces oxidative stress, and promotes apoptosis in KGN cells.

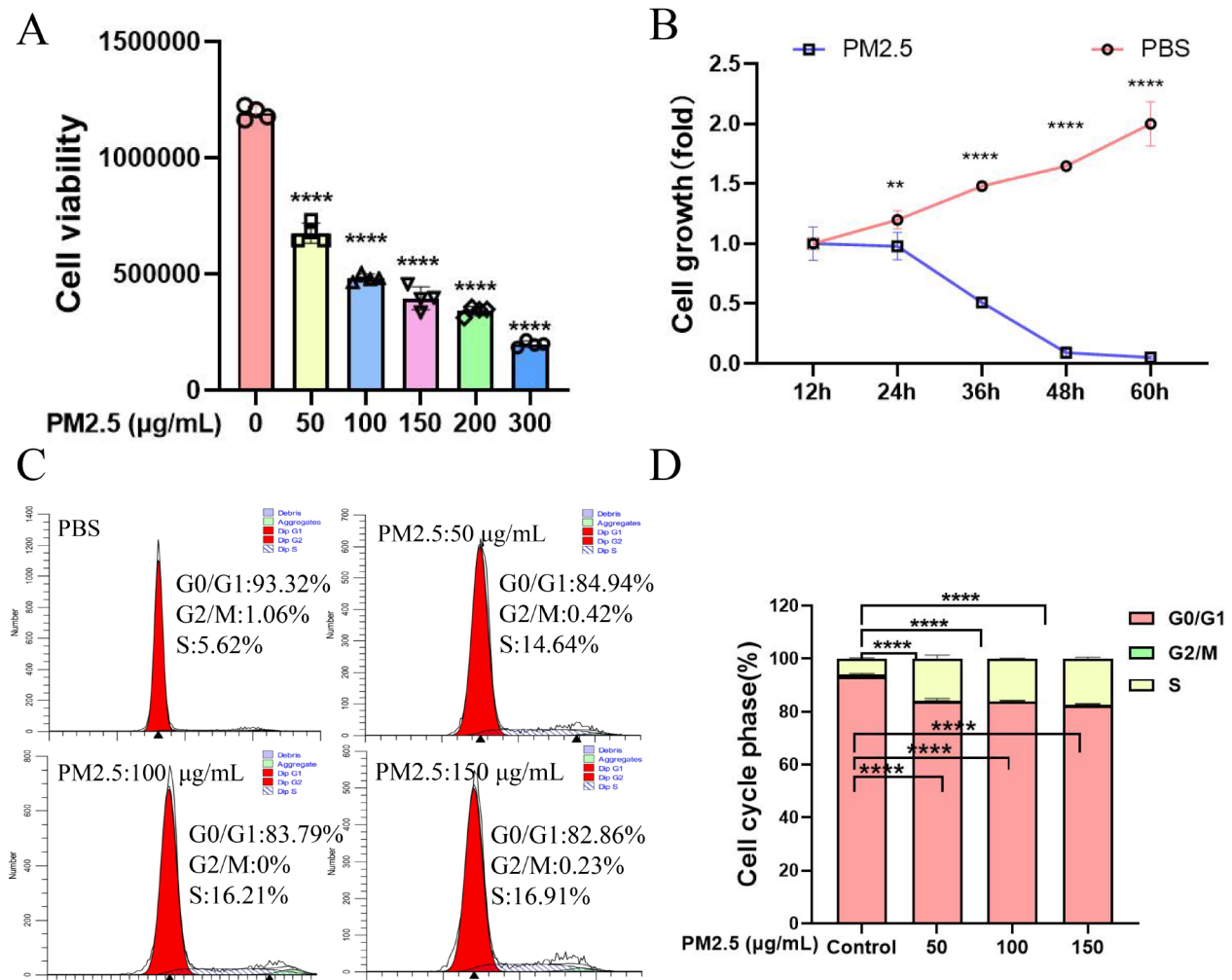


**Fig. 2** Effects of PM2.5 exposure on cell viability and cell cycle in KGN cells. **(A)** With the increase of PM2.5 concentration, cell viability decreased significantly ( $n=4$ ). **(B)** Under the treatment of PM2.5 (100  $\mu\text{g/mL}$ ), as time progresses, cell viability decreases. ( $n=4$ ). **(C-D)** Flow cytometry analysis of KGN cell cycles ( $n=3$ ). \* $P < 0.05$ , \*\* $P < 0.01$ , \*\*\*\* $P < 0.001$ , \*\*\*\*\* $P < 0.0001$

### PM2.5 treatment increased the levels of inflammatory cytokine in vitro via knockdown ATF3

Previous studies have shown that ATF3 suppresses cigarette-induced IL-6 and IL-8 expression by inhibiting the activation of Nuclear Factor kappa B (NF- $\kappa$ B) [24]. RNA-seq data revealed that ATF3 expression was upregulated in response to PM2.5 stimulation (Fig. 4A). This upregulation was consistently observed at the protein level as well (Fig. 4B). We further validated these findings using Enzyme-Linked Immunosorbent Assay (ELISA) to measure inflammatory cytokines. Knockdown of ATF3 led to a significant increase in IL-1, TNE, and IL-6 levels in the supernatant (Fig. 4C-E). In summary, PM2.5 may induce inflammatory responses in KGN cells through an ATF3-mediated pathway.

### Knockdown of ATF3 enhances the apoptosis rate induced by PM2.5 in KGN cells

To explore the roles of ATF3 in PM2.5-induced damage on KGN cells, we tested the effects of PM2.5 on KGN cells after knocking down ATF3. Our results showed a gradual decrease in KGN cell activity under consistent PM2.5 treatment after ATF3 knockdown (Fig. 5A). To further elucidate ATF3's function, we examined the effect of PM2.5 on apoptosis through flow cytometry. The results indicated that apoptosis increased significantly compared to the control group upon ATF3 knockdown (Fig. 5B-C), with a concurrent significant increase in the bcl-2 associated X protein (BAX)/ B-cell lymphoma 2 (BCL2) protein ratio (Fig. 5D). In summary, PM2.5 induces KGN cell apoptosis via the ATF3 pathway. Additionally, KGN cells exposed to PM2.5 for 36 h and treated with MitoSOX™, had ROS levels (Fig. 5E-F). A few words,

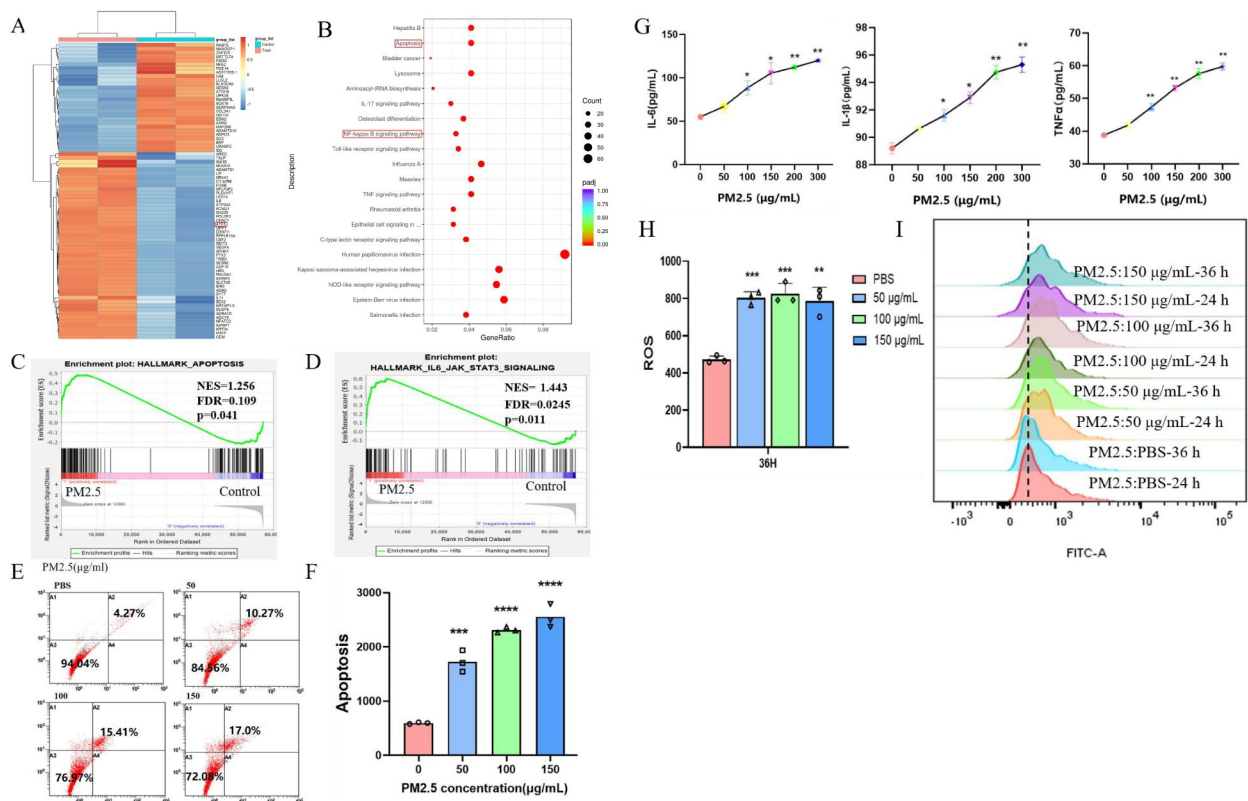


**Fig. 3** PM2.5 exposure triggers oxidative stress and inflammation in vitro. **(A)** Heat map, Cutoff for logFC is 1. The number of up-regulated genes is 181, and down genes is 162. **(B)** Up-gene-KEGG-Analysis. **(C-D)** GSEA results. **(E-F)** Cell apoptosis rates in KGN cells were increased in a dose-dependent manner ( $n=3$ ). **(G)** The expression level of TNF $\alpha$ /IL-1 $\beta$ /IL-6 in cell supernatant was detected by ELISA ( $n=2$ ). **(H-I)** Using the fluorescent dye MitoSOX to study the generation of reactive oxygen species(ROS) ( $n=3$ ). \* $P < 0.05$ , \*\* $P < 0.01$ , \*\*\* $P < 0.001$ , \*\*\*\* $P < 0.0001$

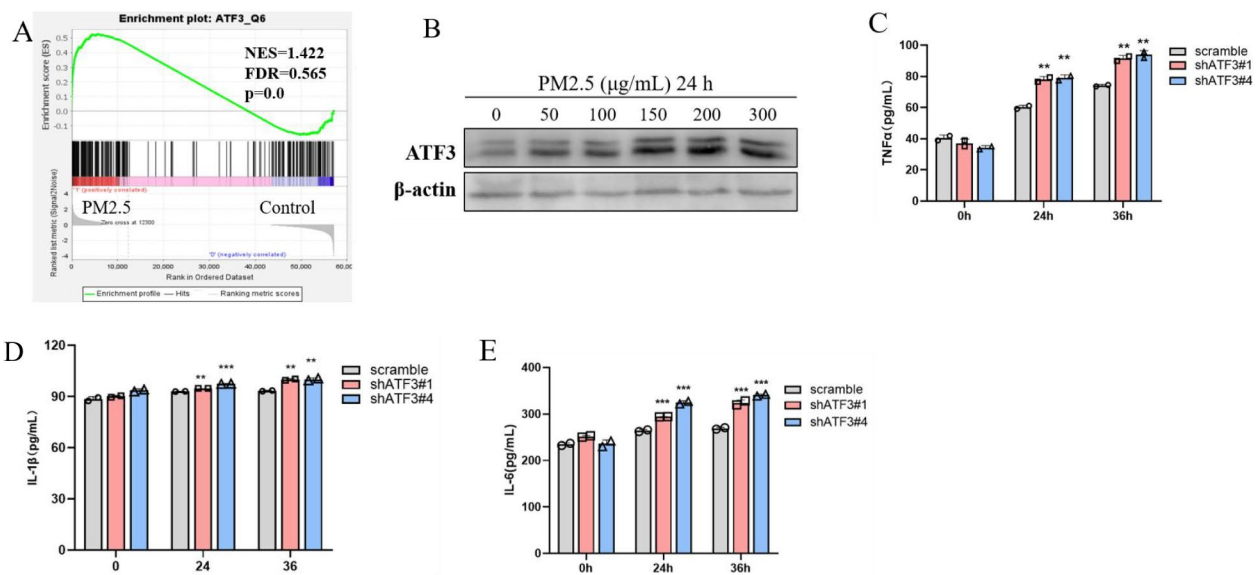


**Fig. 4** PM2.5 treatment increased the levels of inflammatory cytokine in vitro via knockdown ATF3. **(A)** GSEA results of ATF3. **(B)** PM2.5 can increase the expression level of ATF3 protein. **(C-E)** The expression level of TNF $\alpha$ /IL-1 $\beta$ /IL-6 in cell supernatant was detected by ELISA after knockdown ATF3 (PM2.5: 100  $\mu\text{g/mL}$ ;  $n=2$ ). \* $P < 0.05$ , \*\* $P < 0.01$ , \*\*\* $P < 0.001$ , \*\*\*\* $P < 0.0001$

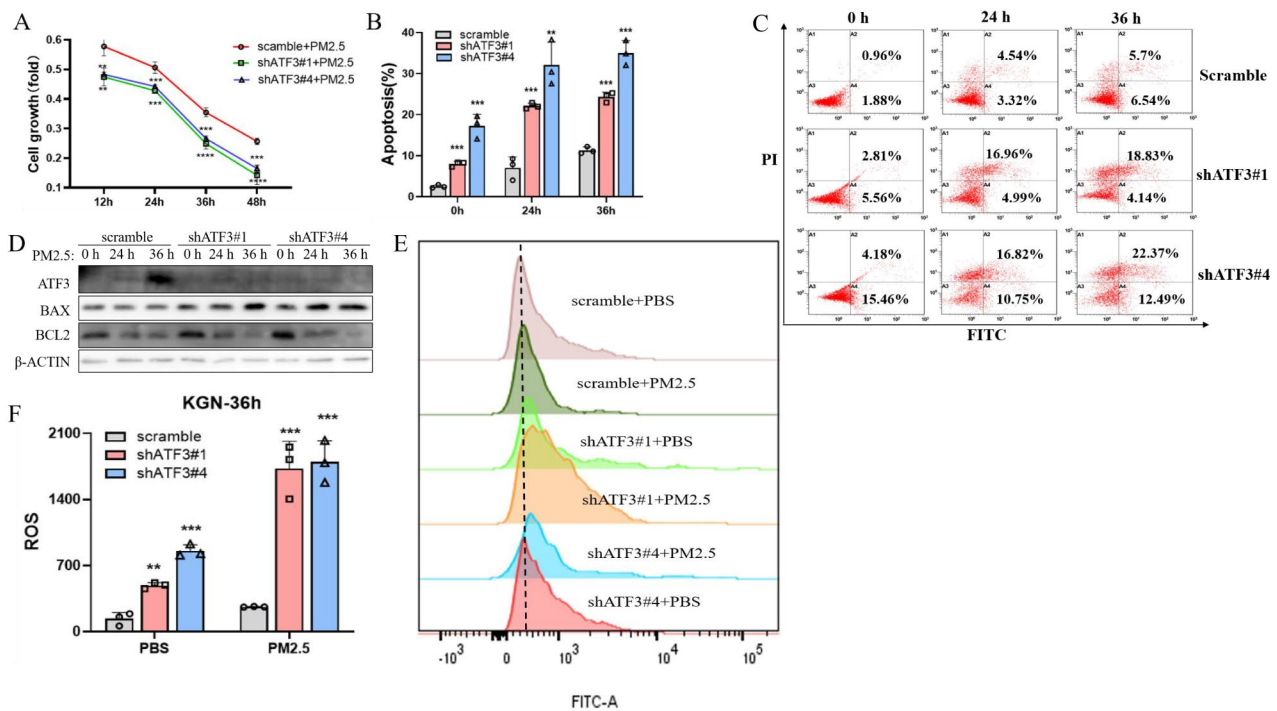


**Fig. 5** Knockdown of ATF3 enhances the apoptosis rate induced by PM2.5 in KGN cells. **(A)** Under the treatment of PM2.5(100  $\mu$ g/mL), the activity of KGN decreased when ATF3 was knocked down ( $n=4$ ). **(B-C)** PM2.5(100  $\mu$ g/mL) causes KGN apoptosis through ATF3. When knocked down ATF3, cell apoptosis rate was significantly increased compared to control ( $n=3$ ). **(D)** On the basis of ATF3 knockdown, PM2.5(100  $\mu$ g/mL) can increase the expression level of apoptotic protein Bax/BCL-2 ratio. **(E-F)** When the ATF3 knockdown, PM2.5(100  $\mu$ g/mL) can aggravate ROS formation in KGN ( $n=3$ ). \* $P < 0.05$ , \*\* $P < 0.01$ , \*\*\* $P < 0.001$ , \*\*\*\* $P < 0.0001$

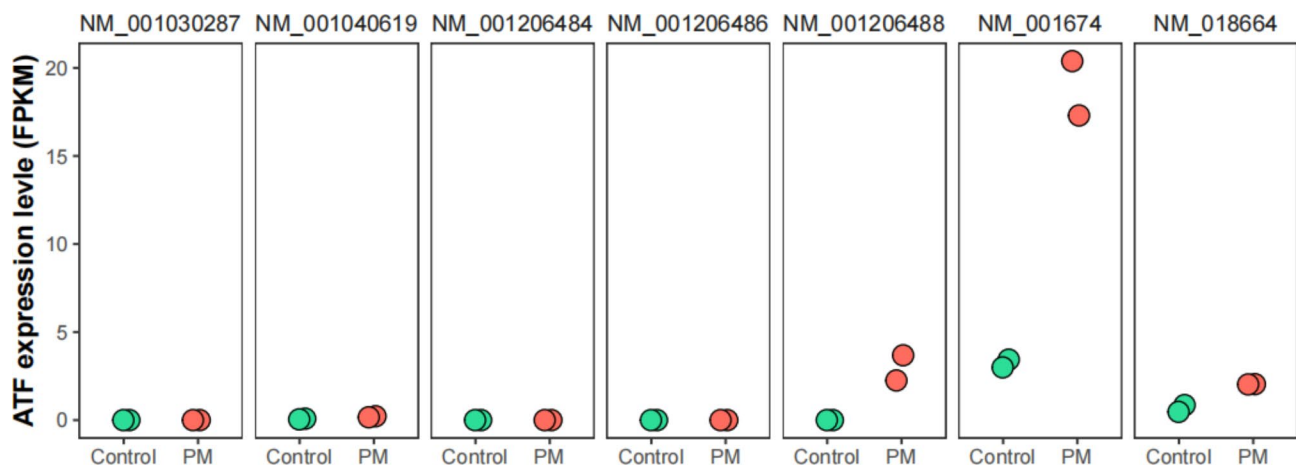


**Fig. 6** ATF3 has several different splice variants

PM2.5 induces oxidative stress levels and apoptosis in KGN cells through the ATF3 pathway.

#### ATF3 has several different splice variants that have substantial differences in function

We analyzed RNA-seq data to that ATF3 splice variants show relevant changes (Fig. 6). Following PM2.5 exposure, the expression level of ATF3 increased, with three splice variants showing changes: NM-001206488,

NM-001674, and NM-018664. Among them, NM-001674 exhibited the most significant change. ATF3 NM-001674 is typically regarded as a negative feedback regulator of the stress response. It is rapidly upregulated when cells experience stress, such as oxidative stress or stimulation by inflammatory factors, and it limits excessive inflammation by suppressing the expression of pro-inflammatory genes. ATF3 can interact with other transcription factors, such as NF- $\kappa$ B, to inhibit the

expression of pro-inflammatory cytokines like IL-6 and TNF- $\alpha$ , thereby mitigating the inflammatory response.

## Discussion

PM2.5-induced ovarian injury is primarily characterized by mitochondrial function in ovarian cells. Previous studies have revealed that PM2.5 can induce ovarian injury through intracellular changes including oxidative stress, inflammation, and apoptotic autophagy-related process [25]. Nevertheless, the precise mechanism of PM2.5-induced damage to ovarian granulosa cells remains unclear. In this study, we discovered that ATF3 is involved in PM2.5-induced inflammation and apoptosis in ovarian granulosa cells.

Most researchers acknowledge that PM2.5 can cause various types of cell death, including autophagy, scorching, necrosis, and apoptosis. In the respiratory system, Dornhof confirmed that chronic PM2.5 exposure promotes lysosome instability, leading to the apoptosis of bronchial epithelial adenocarcinoma BEAS-2B cells via the MAPK signaling pathway [26]. PM2.5 exacerbates mitochondrial damage, leading to increased apoptosis of cardiomyocytes, which accelerates the progression of atherosclerotic plaque formation [27, 28]. Our research illuminates that co-cultivation of PM2.5 with ovarian granulosa cells in vitro cause activity defect and apoptosis in a concentration-dependent manner. Further experiments show that ATF3 knockdown increases the apoptosis rate of ovarian granulosa cells, confirming that ATF3 protects cells from PM2.5-induced damage. However, we speculated that although ATF3 acts as a protector, its function is insufficient to completely counteract PM2.5 damage, making apoptosis inevitable. In future research, we plan to upregulate key proteins in the endogenous ATF3 signaling pathway to assess their effects on PM2.5 exposure in the reproductive system.

In this experiment, we observed ovarian tissue from mice exposed to PM2.5 using HE staining. We figured out that in the chronic exposure group, ovarian inflammation increased, thus raising the risk of follicular atresia. At the same time, ROS levels increased following PM2.5 exposure in the in vitro experiments. Leclercq's research indicates that PM2.5 reduce cell activity by impairing mitochondrial function in bronchial epithelial cells, which may lead to chronic obstructive diseases in lungs [29]. Jin figured out that PM2.5 induced apoptosis in embryonic stem cells by inhibiting the ROS-mediated nuclear factor erythroid 2-related factor 2 pathway (Nrf2), which can be mitigated by N-acetylcysteine [30]. We explored several potential factors underlying PM2.5-induced apoptosis in ovarian granulosa cells, including altered mitochondrial function and an imbalanced antioxidant system that lead to inflammatory reactions damaging cellular activity. Based on our results,

we hypothesize that antioxidant drugs could mitigate PM2.5-induced damage to the ovary. Previous studies have shown that ATF3 exhibits varying effects depending on the type of stimulation. Yan showed that in ATF3 $^{-/-}$  mice, the NF- $\kappa$ B and AP-1 pathways were activated, leading to increased expression of IL-6 and CXCL2 upon exposure to PM2.5<sup>22</sup>. ATF3 can block the NF- $\kappa$ B signaling pathway and inhibit the secretion of IL-6 and IL-8 in response to cigarette smoke [24]. Previous studies have indicated that most critical regulators of ATF3 in the innate immune response can activate the NF- $\kappa$ B signaling pathway while inhibiting the secretion of inflammatory factors. This mechanism indirectly protects immune system homeostasis against inflammation, a finding also supported by our experimental results [31]. In this study, we showed that the inflammatory factors in ovarian granulosa cells, such as TNF- $\alpha$ , IL-1 $\beta$ , and IL-6 induced are dose-dependent in response to PM2.5 exposure. Sequencing analysis revealed that the expression of the ATF3 transcription factor increased with PM2.5 stimulation, while inflammatory factor levels also rose following ATF3 knockdown. This indicates that ATF3 inhibits PM2.5-induced inflammation in ovarian granulosa cells.

This study proposed that ATF3 is a key regulator of apoptosis and PM2.5-induced pro-inflammatory gene expression. The results show that ATF3 is a crucial target for developing interventions against PM2.5-related apoptosis and inflammation, such as modulating endogenous ATF3 or using antioxidants. ATF3-targeted treatments could potentially mitigate PM2.5-induced health damage.

## Materials and methods

### PM2.5 sample collection

PM2.5 samples were collected in Gulou District, Fuzhou City, using a Thermo Scientific GUV-15-H-1 large flow sampler equipped with a G1200-41 PM2.5 sampling head and a quartz fiber membrane (Whatman, USA) at a flow rate of 1.13 m<sup>3</sup>/min. Before sampling, the fiber membrane was calcined at 450 °C for 5 h in a Maboiler furnace to remove any residual organic matter. The fiber membrane was replaced every 24 h. The PM2.5-collecting fiber membrane was cut into 1 cm $\times$ 1 cm pieces, immersed in ultrapure water, placed in an ultrasonic oscillator, shaken at 4 °C for 2 h and then filtered through eight layers of sterile gauze. The filtered liquid was added to a sterile centrifuge tube, centrifuged at low temperature and high speed (4 °C, 12,000 rpm, 30 min), and the supernatant was removed. The precipitates were then dried in a vacuum freeze-dryer for 12 h and stored at 4 °C for later use. The PM2.5 exposure concentration standard was based on the 24-hour average annual concentration limit (35.75  $\mu$ g/m<sup>3</sup>) from the People's Republic of China Ambient Air Quality Standard (GB3095-2012) and the Ambient Air Quality Index (AQI) Technical

Regulations (Trial). Values exceeding  $150 \mu\text{g}/\text{m}^3$  were classified as heavy pollution. PM<sub>2.5</sub> powder was weighed and exposed to ultraviolet irradiation for 1 h on an ultraclean bench. Phosphate-buffered saline (PBS) was added to achieve the optimal concentration and then sterilized for later use.

#### Mouse model for PM<sub>2.5</sub> exposure

A total of 30 healthy SPF female SD mice, each weighing approximately 50 g, were obtained from the Animal Medical Center of Comparative Medicine Laboratory Department of the Ninth Hospital with the production license No: SCXK (Shanghai) 2017-0001. After a seven-day adaptation period, the 30 SD mice were randomly divided into three groups of 10: the control group, the PM<sub>2.5</sub> low-dose group, and the PM<sub>2.5</sub> high-dose group. The mice received PM<sub>2.5</sub> suspension via airway infusion once every 3 days. The exposure doses for the mouse model were based on the 24-hour average PM<sub>2.5</sub> concentration standards in China. The low-dose group was exposed to  $35 \mu\text{g}/\text{m}^3$ , while the high-dose group was exposed to  $150 \mu\text{g}/\text{m}^3$ . The exposure dose was calculated based on the ventilation and lung deposition rates of healthy adult mice, with the low dose being  $3.9 \mu\text{L}$  and the high dose  $16.65 \mu\text{L}$ . The concentration of the suspension was  $2 \mu\text{g}/\mu\text{L}$ . After five months of PM<sub>2.5</sub> airway infusion, castration surgery was performed, and the ovaries were carefully sectioned for subsequent hematoxylin and eosin (H&E) staining.

#### Histology

Ovarian tissue of mice was fixed in 4% paraformaldehyde overnight, dehydrated using ethanol gradient, and embedded in paraffin. H&E staining (Boster, Wuhan, China) was performed on Serial 5- $\mu\text{m}$  ovary sections mounted on glass slides. The tissue sections were examined under a microscope.

#### Cell culture and treatment

The ovarian granulosa cell line (KGN cells) was purchased from Procell (Wuhan, China) and confirmed as ovarian granulosa cells. KGN cells were cultured in DMEM/F12 (Procell, China), while HEK293T cells were cultured in DMEM (BasalMedia, China). The culture medium was supplemented with 1% Penicillin-Streptomycin solution (100 U/mL; Bioss, China) and 10% fetal bovine serum (FBS; Gemini, USA). All cells were incubated at 37°C in a 5% CO<sub>2</sub> atmosphere.

#### Cell viability analysis

A 6-well white plate was cultured KGN with PM<sub>2.5</sub> concentrations of 0, 50, 100, 150, 200 and 300  $\mu\text{g}/\text{mL}$  (The selection of 100  $\mu\text{g}/\text{mL}$  was based on the reference to China's Ambient Air Quality Standards (GB3095-2012) for

Class I and II 24-hour average annual concentration limits ( $35 \mu\text{g}/\text{m}^3$  and  $75 \mu\text{g}/\text{m}^3$ ), as well as the annual average PM<sub>2.5</sub> concentration of  $150 \mu\text{g}/\text{m}^3$  reported in Greenpeace's "2015 Annual PM<sub>2.5</sub> Concentration Rankings of 336 Cities in China", and the cell state under each concentration was observed under a microscope. All steps were repeated three times to ensure high repeatability of the experiment.

Cell viability was analyzed by adding PBS supplemented with Cell Titer-Glo (Promega, USA) to the affected cells in 96-well white plates at 0, 12, 24, 36, 48, and 60 h after the addition of PM<sub>2.5</sub> (100  $\mu\text{g}/\text{mL}$ ).

#### Apoptosis analysis

KGN were immersed in PM<sub>2.5</sub>(100  $\mu\text{g}/\text{mL}$ ) suspension for 24 and 36 h, then directly collected into centrifuge tubes and centrifuged. The precipitated cells were washed once with incubation binding buffer, then 500  $\mu\text{L}$  of buffer was added for resuspension. The suspended cells were incubated with fluorescent Annexin V-FITC (Biolegend, USA) solution for 15 min at 4 °C, avoiding any exposure to light. Fluorescent Propidium Iodide (PI, Sangon Biotech, China) was then added and incubated for 30 min before flow cytometry analysis. The flow cytometer was set with an excitation wavelength of 488 nm to detect Fluorescein isothiocyanate (FITC) fluorescence signals using a 515 nm passband filter, while a filter with a wavelength greater than 560 nm was used to detect PI.

#### Cell cycle analysis

The KGN were co-cultured with PM<sub>2.5</sub> (100  $\mu\text{g}/\text{mL}$ ) for 24 h, then directly collected into a centrifugal tube. The cells were washed twice and then mixed with anhydrous ethanol and PBS in a 7:3 ratio. The mixture was slowly resuspended and fixed overnight at 4 °C. The cells were stained with PI solution and incubated at room temperature. The cell cycle was identified using flow cytometry and the data were processed with FlowJo-10 software.

#### Western blot analysis

KGN cells were washed twice with pre-cooled PBS, followed by the addition of RIPA buffer in the appropriate ratio. Proteins were separated by SDS-PAGE based on their molecular weight and then transferred to a PVDF membrane, which was subsequently blocked with 5% skimmed milk. The membrane was incubated overnight at 4 °C with various primary antibodies. Afterward, the membrane was incubated with the corresponding secondary antibody. The antibodies used were as follows: anti-ATF3 (Abcam, USA, 1:1000), anti-BAX (Cell Signaling, USA, 1:1000), anti-BCL2 (Cell Signaling, USA, 1:1000), anti-GAPDH (SAB, China, 1:10000), and anti- $\beta$ -ACTIN (SAB, China, 1:10000).



**Table 1** Primer sequence of ATF3

Name	Sequence
shATF3#1(human)	CCGGGCTGAAGCTGAAGGCTCAGATTCTCG AGAATCTGAGCCTTCAGTTTCAGCTTTTGG CAAAAAGCTGAAGCTGAAGGCTCAGATTCT CGAGAATCTGAGCCTTCAGTTTCAGCCCGG
shATF3#4(human)	CCGGGGACTCCAGAAGATGAGAGAAGCTC GAGTTCTCTCATCTTCTGGAGTCTTTTGG CAAAAAGGACTCCAGAAGATGAGAGAAG TCGAGTTCTCTCATCTTCTGGAGTCCCGG

### Inflammatory cytokines analysis by ELISA

Inflammatory cytokines TNF- $\alpha$ , IL-6, and IL-1 $\beta$  were measured in cell supernatants using Human IL-1 $\beta$  and IL-6 ELISA kits (Multi Science, China) and a Human TNF- $\alpha$  ELISA kit (Boster, China) following the manufacturers' instructions. The preparation of standards and samples followed the instructions provided with each kit. Standard curves for TNF- $\alpha$ , IL-6, and IL-1 $\beta$  were generated, and their concentrations in the samples, assayed in duplicate, were calculated.

### ROS assay

Reactive oxygen species (ROS) were measured after 36 h incubations with PM<sub>2.5</sub> (100  $\mu$ g/mL). The cells were incubated with a MitoSOX working solution containing the DCFH-DA probe (Beyotime, China) for 20 min at 37°C. After incubation, the MitoSOX working solution was removed, and the cells were collected. Finally, resuspended with 500  $\mu$ L of the serum-free medium and measured using FACS. After adding the MitoSOX working solution, it is necessary to avoid light exposure.

### Cell transfection and lentiviral infection

For lentivirus production, lentiviral vectors were co-transfected into HEK293T cells along with packaging vectors psPAX2 (#12260, Addgene) and pMD2.G (#12259, Addgene). The medium was changed 6 h post-transfection. Infectious lentivirus particles were harvested at 48 h after transfection, filtered through 0.45  $\mu$ m and 0.22  $\mu$ M PVDF filters, and subsequently transduced into cells. The knockdown ATF3 primer sequence was designed (Table 1).

### RNA sequencing (RNA-seq)

Sequencing libraries were generated using the NEB-Next® Ultra™ RNA Library Prep Kit for Illumina® (NEB, USA), and index codes were added to assign sequences to each sample according to the manufacturer's recommendations. Total RNA was isolated from KGN cells treated with PM<sub>2.5</sub> (100  $\mu$ g/mL) or from control cells using Trizol reagent. Poly(A) RNA was purified using the PolyTract mRNA Isolation System, and cDNA libraries were then generated. All samples were sequenced using the Novogene HiSeq 4000 platform. Sequence reads were

mapped to the human genome (hg38) using the Novogene sequence analysis pipeline. Average gene expression values (FPKM > 30) from three independent studies were used for the subsequent analysis.

### Supplementary Information

The online version contains supplementary material available at <https://doi.org/10.1186/s13048-024-01539-5>.

Supplementary Material 1

Supplementary Material 2

Supplementary Material 3

Supplementary Material 4

Supplementary Material 5

Supplementary Material 6

### Author contributions

XD Z, X W, and H J H wrote the main manuscript; XD Z and H L prepared Figs. 1B, 2, 3E-G and 4B-E, and Fig. 5A-D; HH W prepared Fig. 1A; X W prepared Figs. 3H-I and 5E-F, and DD W prepared Figs. 3A-D and 4A. All authors reviewed the manuscript.

### Funding

This work was supported by grants from the National Natural Science Foundation of China (No. 81771547) and Natural Science Foundation of Fujian Province (No. 2020J011145).

### Data availability

No datasets were generated or analysed during the current study.

### Declarations

#### Competing interests

The authors declare no competing interests.

#### Institutional review board statement

The animal study protocol was approved by the Institutional Review Board (LACUC-2018-07).

Received: 12 June 2024 / Accepted: 18 October 2024

Published online: 05 November 2024

### References

- Linou N, Beagley J, Huikuri S, Renshaw N. Air pollution moves up the global health agenda. *BMJ* Nov. 2018;27:363:k4933.
- Guo S, Hu M, Zamora ML, et al. Elucidating severe urban haze formation in China. *Proc Natl Acad Sci U S Dec*. 2014;9(49):17373–8.
- Zhang R, Wang G, Guo S, et al. Formation of urban fine particulate matter. *Chem Rev* May. 2015;27(10):3803–55.
- Li D, Li Y, Li G, Zhang Y, Li J, Chen H. Fluorescent reconstitution on deposition of PM<sub>2.5</sub> in lung and extrapulmonary organs. *Proc Natl Acad Sci U S Feb*. 2019;12(7):2488–93.
- Zhou Y, Ma J, Wang B, et al. Long-term effect of personal PM<sub>2.5</sub> exposure on lung function: a panel study in China. *J Hazard Mater Jul*. 2020;5:393:122457.
- Mahalingaiah S, Missmer SE, Cheng JJ, Chavarro J, Laden F, Hart JE. Perinatal air pollution exposure and menstrual disorders. *Hum Reprod Mar*. 2018;1(3):512–9.
- Zhou S, Xi Y, Chen Y, et al. Ovarian Dysfunction Induced by Chronic whole-body PM<sub>2.5</sub> exposure. *Small Aug*. 2020;16(33):e2000845.
- Mahalingaiah S, Hart JE, Laden F, et al. Adult air pollution exposure and risk of infertility in the nurses' Health Study II. *Hum Reprod Mar*. 2016;31(3):638–47.

9. Carre J, Gatimel N, Moreau J, Parinaud J, Leandri R. Does air pollution play a role in infertility? A systematic review. *Environ Health Jul.* 2017;28(1):82.
10. Naav A, Erlandsson L, Isaxon C, et al. Urban PM2.5 induces Cellular toxicity, hormone dysregulation, oxidative damage, inflammation, and mitochondrial interference in the HRT8 trophoblast cell line. *Front Endocrinol (Lausanne).* 2020;11:75.
11. Klepac P, Locatelli I, Korosec S, Kunzli N, Kušec A. Ambient air pollution and pregnancy outcomes: a comprehensive review and identification of environmental public health challenges. *Environ Res Nov.* 2018;167:144–59.
12. Jie Yin, Weiwei Xia, Yuanyuan Li, Chuchu Guo, Yue Zhang, Songming Huang, Zhanjun and Jia, Aihua Zhang. COX-2 mediates PM2.5-induced apoptosis and inflammation in vascular endothelial cells-17. *Am J Translational Res.* 2017.
13. Cao J, Qin G, Shi R, et al. Overproduction of reactive oxygen species and activation of MAPKs are involved in apoptosis induced by PM2.5 in rat cardiac H9c2 cells. *J Appl Toxicol Apr.* 2016;36(4):609–17.
14. Li J, Zhou Q, Liang Y, et al. miR-486 inhibits PM2.5-induced apoptosis and oxidative stress in human lung alveolar epithelial A549 cells. *Ann Transl Med Jun.* 2018;6(11):209.
15. Zhao C, Wang Y, Su Z, et al. Respiratory exposure to PM2.5 soluble extract disrupts mucosal barrier function and promotes the development of experimental asthma. *Sci Total Environ Aug.* 2020;15:730:139145.
16. Iezaki T, Ozaki K, Fukasawa K, et al. ATF3 deficiency in chondrocytes alleviates osteoarthritis development. *J Pathol Aug.* 2016;239(4):426–37.
17. Bambouskova M, Gorvel L, Lampropoulou V, et al. Electrophilic properties of itaconate and derivatives regulate the I $\kappa$ B $\beta$ -ATF3 inflammatory axis. *Nat Apr.* 2018;556(7702):501–4.
18. Zhao J, Li X, Guo M, Yu J, Yan C. The common stress responsive transcription factor ATF3 binds genomic sites enriched with p300 and H3K27ac for transcriptional regulation. *BMC Genomics May.* 2016;4:17:335.
19. Zhou H, Li N, Yuan Y, et al. Activating transcription factor 3 in cardiovascular diseases: a potential therapeutic target. *Basic Res Cardiol Aug.* 2018;9(5):37.
20. Rohini M, Haritha Menon A, Selvamurugan N. Role of activating transcription factor 3 and its interacting proteins under physiological and pathological conditions. *Int J Biol Macromol Dec.* 2018;120(Pt A):310–7.
21. Koichi Inoue, Takeru Zama, Takahiro Kamimoto, Ryoko Aoki, Yasuo Ikeda, Hiroshi Kimura and Masatoshi Hagiwara. TNF $\alpha$ -induced ATF3 expression is bidirectionally regulated by the JNK and ERK pathways in vascular endothelial cells. 2004.
22. Yan F, Wu Y, Liu H, Wu Y, Shen H, Li W. ATF3 is positively involved in particulate matter-induced airway inflammation in vitro and in vivo. *Toxicol Lett May.* 2018;1:287:113–21.
23. Zhou J. Abnormal ovarian function in SD rats induced by exposure to atmospheric particulate matter PM2.5 [D]. Fujian Medical University, 2016.
24. Wu YP, Cao C, Wu YF, et al. Activating transcription factor 3 represses cigarette smoke-induced IL6 and IL8 expression via suppressing NF- $\kappa$ B activation. *Toxicol Lett Mar.* 2017;15:270:17–24.
25. Liao BQ, Liu CB, Xie SJ, et al. Effects of fine particulate matter (PM2.5) on ovarian function and embryo quality in mice. *Environ Int Feb.* 2020;135:105338.
26. Dornhof R, Maschowski C, Osipova A, et al. Stress fibers, autophagy and necrosis by persistent exposure to PM2.5 from biomass combustion. *PLoS ONE.* 2017;12(7):e0180291.
27. Yang X, Feng L, Zhang Y, et al. Cytotoxicity induced by fine particulate matter (PM2.5) via mitochondria-mediated apoptosis pathway in human cardiomyocytes. *Ecotoxicol Environ Saf Oct.* 2018;161:198–207.
28. Liu J, Liang S, Du Z, et al. PM2.5 aggravates the lipid accumulation, mitochondrial damage and apoptosis in macrophage foam cells. *Environ Pollut Jun.* 2019;249:482–90.
29. Leclercq B, Kluzza J, Antherieu S, et al. Air pollution-derived PM2.5 impairs mitochondrial function in healthy and chronic obstructive pulmonary diseased human bronchial epithelial cells. *Environ Pollut Dec.* 2018;243(Pt B):1434–49.
30. Jin L, Ni J, Tao Y, et al. N-acetylcysteine attenuates PM2.5-induced apoptosis by ROS-mediated Nrf2 pathway in human embryonic stem cells. *Sci Total Environ May.* 2019;20:666:713–20.
31. Kwon JW, Kwon HK, Shin HJ, Choi YM, Anwar MA, Choi S. Activating transcription factor 3 represses inflammatory responses by binding to the p65 subunit of NF- $\kappa$ B. *Sci Rep Sep.* 2015;28:5:14470.

#### Publisher's note

Springer Nature remains neutral with regard to jurisdictional claims in published maps and institutional affiliations.